Structure-based design of hepatitis C virus E2 glycoprotein improves serum binding and cross-neutralization

Brian G. Pierce[1,2#], Zhen-Yong Keck[3#], Ruixue Wang[1], Patrick Lau[3], Kyle Garagusi[1], Khadija Elkholy[1], Eric A. Toth[1], Richard A. Urbanowicz[4,5], Johnathan D. Guest[1,2], Pragati Agnihotri[1,2], Melissa C. Kerzic[1,2], Alexander Marin[1], Alexander K. Andrianov[1], Jonathan K. Ball[4,5], Roy A. Mariuzza[1,2], Thomas R. Fuerst[1,2*], Steven K.H. Foung[3]*

[1]University of Maryland Institute for Bioscience and Biotechnology Research, Rockville, MD 20850, USA

[2]Department of Cell Biology and Molecular Genetics, University of Maryland, College Park, MD 20742, USA

[3]Department of Pathology, Stanford University School of Medicine, Stanford, California 94305, USA

[4]School of Life Sciences, The University of Nottingham, Nottingham, NG7 2RD UK,

[5]NIHR Nottingham Biomedical Research Centre, Nottingham University Hospitals NHS Trust and The University of Nottingham, Nottingham, NG7 2UH UK

#Co-first authors and in order of increasing seniority

*Corresponding authors: sfoung@stanford.edu (SKHF); tfuerst@umd.edu (TRF)

Abstract

An effective vaccine for hepatitis C virus (HCV) is a major unmet need, and it requires an antigen that elicits immune responses to key conserved epitopes. Based on structures of antibodies targeting HCV envelope glycoprotein E2, we designed immunogens to modulate the structure and dynamics of E2 and favor induction of bNAbs in the context of a vaccine. These designs include a point mutation in a key conserved antigenic site to stabilize its conformation, as well as redesigns of an immunogenic region to add a new N-glycosylation site and mask it from antibody binding. Designs were experimentally characterized for binding to a panel of human monoclonal antibodies (HMAbs) and the coreceptor CD81 to confirm preservation of epitope structure and preferred antigenicity profile. Selected E2 designs were tested for immunogenicity in mice, with and without hypervariable region 1, which is an immunogenic region associated with viral escape. One of these designs showed improvement in polyclonal immune serum binding to HCV pseudoparticles and neutralization of isolates associated with antibody resistance. These results indicate that antigen optimization through structure-based design of the envelope glycoproteins is a promising route to an effective vaccine for HCV.

Importance

Hepatitis C virus infects approximately 1% of the world's population, and no vaccine is currently available. Due to the high variability of HCV and its ability to actively escape the immune response, a goal of HCV vaccine design is to induce neutralizing antibodies that target conserved epitopes. Here we performed structure-based design of several epitopes of the HCV E2 envelope glycoprotein to engineer its antigenic properties. Designs were tested in vitro and in vivo, demonstrating alteration of the E2 antigenic profile in several cases, and one design led to improvement of cross-neutralization of heterologous viruses. This represents a proof of concept that rational engineering of HCV envelope glycoproteins can be used to modulate E2 antigenicity and optimize a vaccine for this challenging viral target.

Introduction

Hepatitis C virus (HCV) infection is a major global disease burden, with 71 million individuals, or approximately 1% of the global population, chronically infected worldwide, and 1.75 million new infections per year (1). Chronic HCV infection can lead to cirrhosis and hepatocellular carcinoma, the leading cause of liver cancer, and in the United States HCV was found to surpass HIV and 59 other infectious conditions as a cause of death (2). While the development of direct-acting antivirals has improved treatment options considerably, several factors impede the effective use of antiviral treatment such as the high cost of antivirals, viral resistance, occurrence of reinfections after treatment cessation, and lack of awareness of infection in many individuals since HCV infection is considered a silent epidemic. Therefore, development of an effective preventative vaccine for HCV is necessary to reduce the burden of infection and transmission, and for global elimination of HCV (3).

Despite decades of research resulting in several HCV vaccine candidates tested in vivo and in clinical trials (4, 5), no approved HCV vaccine is available. There are a number of barriers to the development of an effective HCV vaccine, including the high mutation rate of the virus which leads to viral quasi-species in individuals and permits active evasion of T cell and B cell responses (6). Escape from the antibody response by HCV includes mutations in the envelope glycoproteins, as observed in vivo in humanized mice (7), studies in chimpanzee models (8), and through analysis of viral isolates from human chronic infection (9). This was also clearly demonstrated during clinical trials of a monoclonal antibody, HCV1, which in spite of its targeting a conserved epitope on the viral envelope, failed to eliminate the virus, as viral variants

with epitope mutations emerged under immune pressure and dominated the rebounding viral populations in all treated individuals (10, 11).

There have been a number of successful structure-based vaccine designs for variable viruses such as influenza (12, 13), HIV (14, 15), and RSV (16, 17) where rationally designed immunogens optimize presentation of key conserved epitopes, mask sites using N-glycans, or stabilize conformations or assembly of the envelope glycoproteins. Recent studies have reported use of several of these strategies in the context of HCV glycoproteins, including removal or modification of N-glycans to improve epitope accessibility (18, 19), removal of hypervariable regions (18, 20, 21), or presentation of key conserved epitopes on scaffolds (22, 23). However, such studies have been relatively limited compared with other viruses, in terms of design strategies employed and number of designs tested, and immunogenicity studies have not shown convincing improvement of glycoprotein designs over native glycoproteins in terms of neutralization potency or breadth (18, 21), with the possible exception of an HVR-deleted high molecular weight form of the E2 glycoprotein that was tested in guinea pigs (20).

Here we report the generation, characterization, and in vivo immunogenicity of novel structure-based designs of the HCV E2 glycoprotein, which is the primary target of the antibody response to HCV and a major vaccine target. Designs were focused on antigenic domain D, which is a key region of E2 targeted by broadly neutralizing antibodies (bNAbs) that are resistant to viral escape (24), as well as antigenic domain A, which is targeted by non-neutralizing antibodies (25, 26). Based on the intrinsic flexibility of the neutralizing face of E2 (27), which includes antigenic domain D, and on the locations of bNAb epitopes to this domain (24), we identified a

structure-based design substitution to reduce the mobility of that region and preferentially form the bnAb-bound conformation. We also tested several substitutions to hyperglycosylate and mask antigenic domain A located in a unique region on the back layer of E2, as determined by fine epitope mapping (28), which represents an approach that has been applied to mask epitopes in influenza (29) and HIV (30) glycoproteins. Designs were tested for antigenicity using a panel of monoclonal antibodies (mAbs), and selected designs were tested individually and as combinations for in vivo immunogenicity. Assessment of immunized sera revealed that certain E2 designs yielded improvements in serum binding to recombinant HCV particles, as well as viral cross-neutralization, while maintaining serum binding to soluble E2 glycoprotein and key epitopes. This provides a proof-of-concept that rational design of HCV glycoproteins can lead to improvements in immunogenicity and neutralization breadth.

Results

Structure-based design of E2

We utilized two approaches to design variants of the E2 glycoprotein to improve its antigenicity and immunogenicity (**Figure 1**). For one approach, we used the previously reported structure of the affinity matured bnAb HC84.26.5D bound to its epitope from E2 antigenic domain D (31) (PDB code 4Z0X), which shows the same epitope conformation observed in the context of other domain D human monoclonal antibodies (HMAbs) targeting this site (32). Analysis of this epitope structure for potential proline residue substitutions to stabilize its HMAb-bound conformation identified several candidate sites (**Figure 1A, Table 1**). We selected one of these substitutions, H445P, that is adjacent to core contact residues for domain D located at aa 442-443 (32) for subsequent experimental characterization, due to its position in a region with no secondary structure, and location between residues Y443 and K446 which both make key

antibody contacts in domain D antibody complex structures (31, 32). This also represents a distinct region of the epitope from a substitution that we previously described and tested (A439P) (28).

Another design approach, hyperglycosylation, was utilized to mask antigenic domain A, which is an immunogenic region on the back layer of E2 associated with non-neutralizing antibodies (25, 26, 28). Other antibodies with some binding determinants mapped to this region, including HMAbs AR1A and HEPC46, exhibit limited or weak neutralization (33). NxS (Asparagine-X-Serine) and NxT (Asparagine-X-Threonine) N-glycan sequon substitutions were modeled in Rosetta at solvent-exposed E2 positions in antigenic domain A (**Figure 1B, Table 2**), followed by visual inspection of the modeled E2 mutant structures to confirm exposure of the mutant asparagine residues. This analysis suggested that designs with N-glycans at residues 627 (F627N-V629T), 628 (K628N-R630S), 630 (R630N-Y632T), and 632 (Y632N-G634S) warranted further investigation for effects on antigenicity.

Initial screening of mutant antigenicity using ELISA

We first screened the structure-based designs described above to assess their effects on E2 glycoprotein antigenicity, to confirm that designs preserved the structure of key E2 epitopes, and to disrupt non-neutralizing antigenic domain A HMAb binding in the case of the N-glycan designs. These designs were cloned in E1E2 and assessed using ELISA with a panel of representative HMAbs to antigenic domains A-E (**Figure 2**). Only two HMAb concentrations were tested in this assay, in order to detect major disruptions to HMAb binding, or lack thereof, rather than quantitative measurements. The results indicate that mutant H445P maintained

147 approximately wild-type levels of binding to antibodies, while truncations of HVR1 had varying
148 effects. Binding of domain E HMAb HC33.4, and to a lesser extent HC33.1, was negatively
149 affected by truncation of all of HVR1 (residues 384-410 removed; referred to here as
150 $\Delta HVR1_{411}$), whereas a more limited HVR1 truncation (residues 384-407 removed; referred to
151 here as ΔHVR1) largely restored binding of those bNAbs. The design of ΔHVR1 was based on
152 the observation that residue 408 located within HVR1 affected the binding of HC33.4 but not
153 HC33.1 (34). Likewise, designed N-glycan substitutions showed varying effects on antigenicity,
154 with pronounced reduction of binding for several bNAbs for F627NT (F627N-V629T) and
155 R630NT (R630N-Y632T), while K628NS (K628N-R630S) did not exhibit ablation of domain
156 A antibody binding. In contrast, Y632NS (Y632N-G634S) disrupted binding for both tested
157 domain A HMAbs, with limited loss of binding for other HMAbs. Based on this antigenic
158 characterization, designs H445P, ΔHVR1, and Y632NS were selected for further testing.
159
160 *Biophysical and antigenic characterization of E2 designs*
161 The two candidate structure-based E2 designs H445P, Y632NS, as well as ΔHVR1, were
162 expressed and purified as monomeric soluble E2 (sE2) glycoproteins and tested for
163 thermostability and binding affinity to a panel of HMAbs, as well as the CD81 receptor (**Table**
164 **3**). Pairwise combinations of these designs, and a "Triple" design with all three modifications,
165 were also expressed and tested. As noted previously by others (27), wild-type sE2 was found to
166 exhibit high thermostability (T_m = 84.5 °C in **Table 3**). All designs likewise showed high
167 thermostability, with only minor reductions in T_m, with the exception of combined Triple which
168 had the lowest measured thermostability among the tested E2 mutants (T_m = 76.5 °C).
169

To assess antigenicity of glycoprotein designs, solution binding affinity measurements were performed with Octet using HMAbs that target E2 antigenic domains A, B, D, and E, with two antibodies per domain, as well as the receptor CD81 (**Table 3**). These antibodies have been previously characterized using multiple global alanine scanning studies (28, 35) (CBH-4G, CBH-4D, HC33.1, AR3A, HC33.1), and X-ray structural characterization studies (AR3A, HEPC74, HC84.1, HC33.1, HCV1) (32, 36-39). The HC84.26.WH.5DL is an affinity matured clone of the parental HC84.26 antibody with improved affinity and neutralization breadth over the parental antibody (31). The binding site of CD81 has been mapped to E2 residues in antigenic domains B, D, and E (35), thus CD81 binding provides additional assessment of antigenicity of that E2 supersite (6). Binding experiments with this panel showed nanomolar binding affinities to wild-type sE2, which were largely maintained for sE2 designs. A 10-fold increase in binding affinity of sE2 design H445P for domain D HMAb HC84.26.WH.5DL was observed, showing that this design, located within antigenic domain D, not only maintained affinity, but improved engagement in that case; a steady-state binding fit for that interaction is shown in **Figure 3A**. However, this effect was not observed for combinations of designs including H445P, suggesting possible interplay between designed sites. As expected, domain A hyperglycosylation designs Y632NS, ΔHVR1-Y632NS, and Triple (ΔHVR1-H445P-Y632NS) showed loss of binding (>5-fold for each) to antigenic domain A HMAb CBH-4G (Y632NS-CBH-4G binding measurement is shown in **Figure 3B**), though we did not observe disruption of binding to CBH-4D. Additionally, design ΔHVR1-Y632NS showed moderate (6-fold) loss of CD81 binding, which was not the case for other designs. As domain A HMAbs have distinct, albeit similar, binding determinants on E2 (28), differential effects on domain A antibody binding by Y632NS variants reflect likely differences in HMAb docking footprints on E2.

193 Measurements of glycan occupancy at residue 632 using mass spectroscopy showed partial
194 levels of glycosylation at that site for Y632NS and combinations (**Table 4**), which may be
195 responsible for incomplete binding ablation to the tested antigenic domain A HMAbs. As alanine
196 substitution at Y632 was previously found to disrupt binding of domain A antibodies (28), it is
197 possible that the Y632N amino acid substitution in the Y632NS may be responsible, in addition
198 to partial N-glycosylation, for effects on domain A antibody binding. Regardless, these results
199 suggest at least partial binding disruption and N-glycan masking of this region, supporting
200 testing of those designs as immunogens in vivo.
201
202 *In vivo immunogenicity of E2 designs*
203 Following confirmation of antigenicity, E2 designs were tested in vivo for immunogenicity, to
204 assess elicitation of antibodies that demonstrate potency and neutralization breadth. CD1 mice (6
205 per group) were immunized with H77C sE2 and designs, employing Day 0 prime and followed
206 by three biweekly boosts. Sera were obtained at Day 56 after initial injection (two weeks after
207 the final boost) and tested for binding to H77C sE2 and key conserved epitopes (AS412/Domain
208 E, AS434/Domain D) (**Figure 4**). Peptide epitopes were confirmed for expected monoclonal
209 antibody specificity using ELISA (**Figure 4B**). Endpoint titers demonstrated that sera from mice
210 immunized with E2 designs maintained recognition of sE2 and tested epitopes. Intra-group
211 variability resulted in lack of statistically significant differences in serum binding between
212 immunized groups, however mean titers from ΔHVR1 group were moderately lower than the
213 wild-type sE2 group, and other mutants yielded moderately higher serum binding to the tested
214 epitopes. Notably, design H445P elicited antibodies that robustly cross-reacted with the wild
215 type AS434/Domain D epitope. To assess differential binding to conformational epitopes on E2,

serum binding competition with selected HMAbs was performed (**Figure 5**). The observation of competition in the majority of antisera suggests that elicited antibodies to domain D are to native conformational epitopes, although there were no major differences between immunized groups. Likewise, no substantial differences in serum competition for binding to antigenic domains A or B were detected among immunized groups.

Serum binding to HCV E1E2 and HCV pseudoparticles

For further analysis of immunized serum binding, we tested binding to concentrated recombinant H77C E1E2 and HCV pseudoparticles from H77C and two heterologous genotypes (**Figure 6, Table 5**). While binding to H77 E1E2 resembled binding to H77 sE2, with no apparent difference between immunized groups, we observed notable differences in binding to HCVpps representing H77C, UKNP1.18.1, and J6 for H445P-immunized mice versus mice immunized with wild-type sE2. The difference between J6 HCVpp binding from H445P-immunized mice versus sE2-immunized mice was highly significant ($p \leq 0.0001$, Kruskal-Wallis test). To confirm this difference in HCVpp binding between sE2 and H445P immunized groups, given the relatively low levels of overall titers, H77C HCVpps were concentrated and tested in ELISA for binding to pooled sera from sE2 and H445P immunized mice. This confirmed differences between immunized groups for sera from Day 56, as well as Day 42, which corresponds to three rather than four immunizations (**Figure 7**). To demonstrate native-like E2 and E1E2 assembly of the HCVpps in the context of the ELISA assay, concentrated HCVpps showed binding to monoclonal antibodies that target linear and conformational epitopes on E2 (HCV1, HC84.26.WH.5DL, AR3A) and conformational epitopes on E1E2 (AR4A, AR5A), and did not interact with negative control antibody (CA45) (**Figure 8**). The molecular basis for the

239 differential serum reactivity when using HCVpp versus purified recombinant E1E2 in ELISA is
240 unclear, particularly given that sE2 was used as an immunogen, yet these results collectively
241 provide evidence that H445P may improve targeting of conserved glycoprotein epitopes on the
242 intact HCV virion.
243
244 *Homologous and heterologous serum neutralization*
245 To assess effects of antibody neutralization potency and breadth from E2 designs, we tested
246 serum neutralization of HCVpp representing homologous H77C and six heterologous isolates
247 (**Figure 9**). The heterologous isolates collectively diverge substantially in sequence from H77C
248 and represent neutralization phenotypes ranging from moderately to highly resistant (**Table 5**),
249 with the latter represented by three of the most resistant tested HCVpp from a previous study that
250 performed characterization with a panel of neutralizing monoclonal antibodies (40) (UKNP2.4.1,
251 UKNP4.1.1, UKNP1.18.1). As we found previously with immunization of H77C-based sE2 (19),
252 there was relatively large intra-group variability in neutralization of H77C, and no statistically
253 significant differences between groups were observed. However, ID50 values for individual mice
254 varied less within immunized groups for heterologous isolates. Comparison between groups
255 immunized with sE2 designs and wild-type sE2 showed significantly higher neutralization in
256 some cases. Notably, two resistant isolates had significantly higher neutralization for H445P-
257 immunized sera than wild-type sE2-immunized sera (UKNP1.18.1, J6).
258
259 *Analysis of correlates of immunogenicity and antigenicity*
260 Based on our in vitro and in vivo measurements, we assessed correlations between serum
261 neutralization of different genotypes, serum antigen binding, and antigenicity (**Figure 10**). First,

we performed correlations between immunogenicity measurements for individual murine sera, corresponding to 42 points per dataset. Measurements of HCVpp serum binding were not included in this analysis, due to low and unquantifiable binding measurements for multiple mice for those assays (**Figure 6B-D**). Top correlations between immunogenicity measurements (**Figure 10A**) include serum binding values (EC50) to sE2 versus E1E2 ($r = 0.84$), J6 neutralization (ID50) versus UKNP1.18.1 neutralization ($r = 0.66$), and UKNP2.4.1 neutralization versus UKNP1.18.1 neutralization ($r = 0.51$), all of which were highly significant ($p \leq 0.001$). The latter two correlations highlight shared patterns of neutralization of HCVpp with resistant phenotypes; a plot of UKNP2.4.1 HCVpp ID50 values versus UKNP1.18.1 HCVpp ID50 values is shown in **Figure 10B**.

To assess possible associations between antigenicity and immunogenicity, we calculated correlations between measured binding affinity values for HMAbs and group immunogenicity measurements (endpoint titer or HCVpp ID50). Such analysis has been used by others with other viral antigen designs to examine antigenic properties associated with immunogenicity (16). Top correlations based on significance (p-value) are shown in **Figure 10C**. As with the individual mouse correlation analysis noted above, HCVpp endpoint titers were excluded from this analysis due to insignificant binding values in several groups. As expected due to limited number of data points and limited overall variability in binding affinity measurements (**Table 3**), few correlations between antigenic and immunogenic parameters were highly significant, though binding of domain D HMAb HC84.26.WH.5DL was highly correlated with neutralization of J6 HCVpp ($r = 0.97$, $p = 0.0003$), as well as neutralization of UKNP1.18.1 HCVpp ($r = 0.88$, $p = 0.008$), while anticorrelations were detected for other antibody binding measurements (HEPC74 and HCV1) and HCVpp group neutralization values, at lower significance levels. The high

correlations involving HMAb HC84.26.WH.5DL are not unexpected, based on the higher HMAb binding affinity to the H445P sE2 antigen and higher nAb responses induced by H445P; **Figure 10D** compares UKNP1.18.1 neutralization with HC84.26.WH.5DL binding, where the point corresponding to H445P is in the upper right.

Discussion

In this study, we applied a variety of rational design approaches to engineer the HCV E2 glycoprotein to improve its antigenicity and immunogenicity. One of these approaches, removal of HVR1 (ΔHVR1), has been tested in several recent immunogenicity studies, in the context of E2 (18, 20, 23) and E1E2 (21). In this study, we tested the E2 ΔHVR1 mutant with residues 384-407 removed, which retains residues 408-661 of E2; this is a more conservative truncation than previously tested ΔHVR1 mutants, in order to retain residue 408 which is binding determinant for the HC33.4 HMAb and others (28, 34). Here we found this mutant to not be advantageous from an immunogenicity standpoint, which is in agreement with most other previous immunogenicity studies testing ΔHVR1 mutants (18, 21, 23). Although HVR1 is an immunogenic epitope, its removal from recombinant E2 glycoprotein does not appear to increase homologous or heterologous nAb titers, with the latter suggesting that the level of antibodies targeting conserved nAb epitopes did not increase upon HVR1 removal. Based largely on studies of engineered viruses in cell culture, as summarized in a recent review (41), removal of HVR1 is associated with increased nAb sensitivity and CD81 receptor binding, while a recent study has indicated that HVR1 may modulate viral dynamics and open and closed conformations during envelope breathing (42). Despite its importance in the context of the virion and its dynamics, its

307 removal appears to have a neutral or minimal effect on the immunogenicity of recombinant
308 envelope glycoproteins.
309
310 Another design strategy tested in this study was hyperglycosylation, through structure-based
311 addition of N-glycan sequons to mask antigenic domain A, which is associated with non-
312 neutralizing antibodies (25, 26, 28, 43). The concept of down-modulating immunity to this
313 region was based on the observation that this region is highly immunogenic and may divert
314 antibody responses to bNAb epitopes of lower immunogenicity. Through the efforts of isolating
315 bNAbs to distinct regions on E2 from multiple HCV infected individuals, non-neutralizing
316 antibodies to domain A are consistently identified (personal communication, S. Foung). This
317 strategy has been successfully employed for other glycoprotein immunogens, including for HIV
318 Env SOSIP trimers, where the immunogenic V3 loop was masked with designed N-glycans (30).
319 Surprisingly, some of the designs in this study exhibited an impact on recognition by antibodies
320 targeting antigenic domain D on the front layer of E2, suggesting a possible interplay between
321 the front and back layers of E2, as proposed previously based on global alanine scanning
322 mutagenesis (35). As observed by Ringe et al. in the context of HIV Env (30), the designed E2
323 N-glycan variant tested for immunogenicity in this study (Y632NS) did not show improvements
324 in nAb elicitation. However, its combination with ΔHVR1 did lead to modest improvement in
325 nAb titers against one resistant isolate (UKNP2.4.1; p-value < 0.05), compared with wild-type
326 sE2. Previously we used insect cell expression to alter the N-glycan profile of sE2 versus
327 mammalian cell expressed sE2 (19), and others have recently tested immunogenicity for glycan-
328 deleted E2 and E1E2 variants (18); in neither case was a significant improvement in homologous
329 and heterologous nAb responses observed for immunogens with altered glycans. Collectively,

these results suggest that glycoengineering of E2 or E1E2 represents a more challenging, and possibly less beneficial, avenue for HCV immunogen design, however a report of success by others through insect cell expressed sE2 indicates that altered glycosylation may help in some instances (44).

The designed substitution H445P, which was generated to preferentially adopt the bnAb-bound form in a portion of E2 antigenic domain D that exhibits structural variability (31), showed the greatest level of success, both with regard to improvements in serum binding to homologous and heterologous HCVpp, as well as HCVpp neutralization of heterologous HCVpp. This design lies within a supersite of E2 associated with many broadly neutralizing antibodies (5, 6, 45, 46), and through biophysical characterization and molecular dynamics simulation experiments, others have found that this region is likely quite flexible (27, 47), providing a rationale for stabilizing key residues to engage and elicit bNAbs. Interestingly, a residue adjacent to the site of this design appears to be functionally important, with the Q444R substitution restoring viral infectivity in the context of an HCVpp with a domain E “glycan shift” substitution, N417S (8). The design strategy of utilizing proline residue substitutions to stabilize conformations of viral glycoproteins has been successful for HIV Env (48), respiratory syncytial virus (RSV) F (49), MERS coronavirus spike (50), and recently, the novel coronavirus (SARS-CoV-2) spike (51). The data from this study suggest that this approach is also useful in the context of HCV E2, and possibly E1E2.

This study provides a proof-of-concept for computational structure-based design of the HCV E2 glycoprotein to modulate its antigenicity and immunogenicity. Future studies with the H445P

design include testing of its antigenicity and immunogenicity in the context of HCV E1E2, testing immunogenicity in other animal models, as well as confirmation of its impact on E2 structure through high resolution X-ray structural characterization and additional biophysical characterization. Confirmation of improved elicitation of neutralizing antibodies with a cell-culture based HCV assay (HCVcc), versus the pseudoparticle-based assay (HCVpp) used in this study, can provide further insight into the impact of these and other HCV envelope glycoprotein variants. However, the employment of HCVpp does permit a greater ease in testing against clinical isolates. Furthermore, additional designed proline substitutions in this flexible E2 "neutralizing face" supersite may confer greater improvements in homologous and heterologous nAb elicitation; these can be generated using structure-based design, or with a semi-rational library-based approach, as was used to scan a large set of proline substitutions for HIV Env (52). This study provides a promising design candidate for follow-up studies, underscoring the value of the set of previously determined, though somewhat limited, set of E2-bnAb complex structures. Prospective elucidation of the structure of E2 in complex with additional bNAbs, as well as characterization of the E1E2 complex structure, will facilitate future structure-based design studies to engineer and optimize immunogens for an effective HCV vaccine.

Materials and Methods

Computational modeling and design

Proline substitution designs to stabilize epitopes were modeled as previously described for design of T cell receptor binding loops (53), using a Ramachandran plot server to assess epitope residue backbone conformations for proline and pre-proline conformational similarities (http://zlab.bu.edu/rama)(54), as well as explicit modeling of energetic effects of proline

substitutions using the point mutagenesis mode of Rosetta version 2.3 (55). N-glycan sequon substitutions (NxS, NxT) were modeled using Rosetta (55), followed by modeling of the N-glycan structure using the Glyprot web server (56). Assessment of residue side chain accessible surface areas was performed using NACCESS (57) with default parameters.

Protein and antibody expression and purification

Expression and purification of recombinant soluble HCV E2 (sE2) and designs was performed as previously described (19). Briefly, the sequence from isolate H77C (GenBank accession number AF011751; residues 384–661) was cloned into the pSecTag2 vector (Invitrogen), transfected with 293fectin into FreeStyle HEK293-F cells (Invitrogen), and purified from culture supernatants by sequential HisTrap Ni^{2+}-NTA and Superdex 200 columns (GE Healthcare). For recombinant HCV E1E2 expression, the H77C E1E2 glycoprotein coding region (GenBank accession number AF011751) was synthesized with a modified tPA signal peptide (58) at the N-terminus and cloned into the vector pcDNA3.1+ at the cloning sites of KpnI/NotI (GenScript). Expi293 cells (Thermo Fisher) were used to express the E1E2 glycoprotein complex. In brief, the Expi293 cells were grown in Expi293 medium (ThermoFisher) at 37°C, 125 rpm, 8% CO2 and 80% humidity in Erlenmeyer sterile polycarbonate flasks (VWR). The day before the transfection, 2.0×10^6 viable cells/ml was seeded in a flask and the manufacturer's protocol (A14524, ThermoFisher) was followed for transfection performance. After 72 hours post-transfection, the cell pellets were harvested by centrifuging cells at 3,000 x g for 5 min and the cell pellet were then stored at -80 °C for further processing. Recombinant E1E2 was extracted from cell membranes using 1% NP-9 and purified via sequential Fractogel EMD TMAE (Millipore), Fractogel EMD SO_3^- (Millipore). HC84.26 immunoaffinity, and Galanthus Nivalis

Lectin (GNL, Vector Laboratories) affinity chromatography. Monoclonal antibody HCV1 was provided by Dr. Yang Wang (MassBiologics, University of Massachusetts Medical School), and monoclonal antibodies AR3A, AR4A, and AR5A were provided by Dr. Mansun Law (Scripps Research Institute). All other monoclonal antibodies used in ELISA and binding studies were produced as previously described (24, 25, 59). A clone for mammalian expression of CD81 large extracellular loop (LEL), containing N-terminal tPA signal sequence and C-terminal twin Strep tag, was provided by Joe Grove (University College London). CD81-LEL was expressed through transiently transfection in Expi293F cells (ThermoFisher) and purified from supernatant with a Gravity Flow Strep-Tactin Superflow high capacity column (IBA Lifesciences). Purified CD81-LEL was polished by size exclusion chromatography (SEC) with a Superdex 75 10/300 GL column (GE Healthcare) on an Akta FPLC (GE Healthcare).

ELISA antigenic characterization and competition assays

Cloning and characterization of E2 mutant antigenicity using ELISA was performed as described previously (28). Mutants were constructed in plasmids carrying the 1a H77C E1E2 coding sequence (GenBank accession number AF009606), as described previously (60). All the mutations were confirmed by DNA sequence analysis (Elim Biopharmaceuticals, Inc., Hayward, CA) for the desired mutations and for absence of unexpected residue changes in the full-length E1E2-encoding sequence. The resulting plasmids were transfected into HEK 293T cells for transient protein expression using the calcium-phosphate method. Individual E2 protein expression was normalized by binding of CBH-17, an HCV E2 HMAb to a linear epitope (61). Serum samples at specified dilutions were tested for their ability to block the binding of selected

HCV HMAbs-conjugated with biotin in a GNA-captured E1E2 glycoproteins ELISA, as described (24). Data are shown as mean values of two experiments performed in triplicate.

Biolayer interferometry

The interaction of recombinant sE2 glycoproteins with CD81 and HMAbs in was measured using an Octet RED96 instrument and Ni^{2+}-NTA biosensors (Pall ForteBio). The biosensors were loaded with 5 μg/mL of purified His_6-tagged wild-type or mutant sE2 for 600 seconds. Association for 300 sec followed by dissociation for 300 seconds against a 2-fold concentration dilution series of each antibody was performed. Data analysis was performed using Octet Data Analysis 10.0 software and utilized reference subtraction at 0 nM antibody concentration, alignment to the baseline, interstep correction to the dissociation step, and Savitzky-Golay fitting. Curves were globally fitted based on association and dissociation to obtain K_D values.

Differential scanning calorimetry

Thermal melting curves for monomeric E2 proteins were acquired using a MicroCal PEAQ-DSC automated system (Malvern Panalytical). Purified monomeric E2 proteins were dialyzed into PBS prior to analysis and the dialysis buffer was used as the reference in the experiments. Samples were diluted to 10 μM in PBS prior to analysis. Thermal melting was probed at a scan rate of 90 °C·h^{-1} over a temperature range of 25 to 115 °C. All data analyses including estimation of the melting temperature were performed using standard protocols that are included with the PEAQ-DSC software.

Mass spectrometry

Digestion was performed on 40 μg each of HEK293-derived sE2 glycan sequon substitutions by denaturing using 6 M guanidine HCl, 1 mM EDTA in 0.1 M Tris, pH 7.8, reduced with a final concentration of 20 mM DTT (65 °C for 90 min), and alkylated at a final concentration of 50 mM iodoacetamide (room temperature for 30 min). Samples were then buffer exchanged into 1 M urea in 0.1 M Tris, pH 7.8 for digestion. Sequential digestion was performed using trypsin (1/50 enzyme/protein ratio, w/w) for 18 hours at 37 °C, followed by chymotrypsin (1/20 enzyme:protein, w/w) overnight at room temperature. Samples were then absorbed onto Sep-Pak tC18 columns to remove proteolytic digestion buffer, eluted with 50% acetonitrile/0.1% trifluoroacetic acid (TFA) buffer and concentrated to dryness in a centrifugal vacuum concentrator. The samples were then resuspended in 50 mM Sodium acetate pH 4.5 and incubated with Endo F1, Endo F2, and Endo F3 (QA Bio) at 37 °C for 72 hours to remove complex glycans. LC-UV-MS analyses were performed using an UltiMate 3000 LC system coupled to an LTQ Orbitrap Discovery equipped with a heated electrospray ionization (HESI) source and operated in a top 5 dynamic exclusion mode. A volume of 25 μl (representing 10 μg of digested protein) of sample was loaded via the autosampler onto a C18 peptide column (AdvanceBio Peptide 2.7 um, 2.1 x 150 mm, Agilent part number 653750-902) enclosed in a thermostatted column oven set to 50 °C. Samples were held at 4°C while queued for injection. The chromatographic gradient was conducted as described previously (19). Identification of glycosylated peptides containing the glycan sequon substitution was performed using Byonic software and extracted ion chromatograms used for estimating the relative abundance of the glycosylated peptides in Byologic software (Protein Metrics).

Animal immunization

CD-1 mice were purchased from Charles River Laboratories. Prior to immunization, sE2 antigens were formulated with polyphosphazene adjuvant. Poly[di(carboxylatophenoxy)phosphazene], PCPP (molecular weight 800,000 Da) (62) was dissolved in PBS (pH 7.4) and mixed with sE2 antigen solution at 1:1 (prime) or 1:5 (w/w) (boost immunization) antigen:adjuvant ratio to provide for 50 mcg PCPP dose per animal. The absence of aggregation in adjuvanted formulations was confirmed by dynamic light scattering (DLS): single peak, z-average hydrodynamic diameter – 60 nm. The formation of sE2 antigen – PCPP complex was proven by asymmetric flow field flow fractionation (AF4) as described previously (63). On scheduled vaccination days, groups of 6 female mice, age 7-9 weeks, were injected via the intraperitoneal (IP) route with a 50 μg sE2 prime (day 0) and boosted with 10 μg sE2 on days 7, 14, 28, and 42. Blood samples were collected prior to each injection with a terminal bleed on day 56. The collected samples were processed for serum by centrifugation and stored at -80°C until analysis was performed.

Serum peptide and protein ELISA

Domain-specific serum binding was tested using ELISA with C-terminal biotinylated peptides from H77C AS412 (aa 410-425; sequence NIQLINTNGSWHINST) and AS434 (aa 434-446; sequence NTGWLAGLFYQHK), using 2 μg/ml coating concentration. Recombinant sE2 and E1E2 proteins were captured onto GNA-coated microtiter plates. Endpoint titers were calculated by curve fitting in GraphPad Prism software, with endpoint OD defined as four times the highest absorbance value of Day 0 sera.

HCV pseudoparticle generation

HCV pseudoparticles (HCVpp) were generated as described previously (19), by co-transfection of HEK293T cells with the murine leukemia virus (MLV) Gag-Pol packaging vector, luciferase reporter plasmid, and plasmid expressing HCV E1E2 using Lipofectamine 3000 (Thermo Fisher Scientific). Envelope-free control (empty plasmid) was used as negative control in all experiments. Supernatants containing HCVpp were harvested at 48 h and 72 h post-transfection, and filtered through 0.45 μm pore-sized membranes. Concentrated HCVpp were obtained by ultracentrifugation of 33 ml of filtered supernatants through a 7 ml 20% sucrose cushion using an SW 28 Beckman Coulter rotor at 25,000 rpm for 2.5 hours at 4°C, following a previously reported protocol (26).

HCVpp serum binding

For measurement of serum binding to HCVpp, 100 µL of 0.45 µm filtered HCVpp isolates were directly coated onto Nunc-immuno MaxiSorp (Thermo Scientific) microwells overnight at 4°C. Microwells were washed three times with 300 µL of 1X PBS, 0.05% Tween 20 in between steps. Wells were blocked with Pierce Protein-Free Blocking buffer (Thermo Scientific) for 1 hour. Serum sample dilutions made in blocking buffer were added to the microwells and incubated for 1 hour at room temperature. Abs were detected with secondary HRP conjugated goat anti-mouse IgG H&L (Abcam, ab97023) and developed with TMB substrate solution (Bio-Rad). The reaction was stopped with 2M sulfuric acid. A Molecular Devices M3 plate reader was used to measure absorbance at 450 nm. Endpoint titers were calculated by curve fitting in GraphPad Prism software, with endpoint OD defined as four times the highest absorbance value of Day 0 sera.

HCVpp neutralization assays

For infectivity and neutralization testing of HCVpp, 1.5 x 10^4 Huh7 cells per well were plated in 96-well tissue culture plates (Corning) and incubated overnight at 37 °C. The following day, HCVpp were mixed with appropriate amounts of antibody and then incubated for 1 h at 37 °C before adding them to Huh7 cells. After 72 h at 37 °C, either 100 µl Bright-Glo (Promega) was added to each well and incubated for 2 min or cells were lysed with Cell lysis buffer (Promega E1500) and placed on a rocker for 15 min. Luciferase activity was then measured in relative light units (RLUs) using either a SpectraMax M3 microplate reader (Molecular Devices) with SoftMax Pro6 software (Bright-Glo protocol) or wells were individually injected with 50 µL luciferase substrate and read using a FLUOstar Omega plate reader (BMG Labtech) with MARS software. Infection by HCVpp was measured in the presence of anti-E2 MAbs, tested animal sera, pre-immune animal sera, and non-specific IgG at the same dilution. Each sample was tested in duplicate or triplicate. Neutralizing activities were reported as 50% inhibitory dilution (ID_{50}) values and were calculated by nonlinear curve fitting (GraphPad Prism), using lower and upper bounds (0% and 100% inhibition) as constraints to assist curve fitting.

Statistical comparisons and correlations

P-values between group endpoint titers and group ID_{50} values were calculated using Kruskal-Wallis one-way analysis of variance (ANOVA), with Dunn's multiple comparison test, in Graphpad Prism software. Pearson correlations and correlation significance p-values were calculated in R (www.r-project.org).

Acknowledgements

We thank Joe Grove (University College London) for kindly providing the CD81-LEL expression plasmid. We also thank Verna Frasca (Malvern Panalytical) for performing and analyzing the DSC experiments, and Sneha Rangarajan (University of Maryland IBBR) for useful discussions regarding the antigenic domain D structure. This work was supported in part by National Institute of Allergy and Infectious Diseases/NIH grants R21-AI126582 (BGP, RAM, SKHF), R01-AI132213 (BGP, AKA, RAM, TRF, SKHF), and U19-AI123862 (SKHF).

References

1. WHO. 2017. Global Hepatitis Report 2017. World Health Organization.
2. Ly KN, Hughes EM, Jiles RB, Holmberg SD. 2016. Rising Mortality Associated With Hepatitis C Virus in the United States, 2003-2013. Clin Infect Dis 62:1287-8.
3. Cox AL. 2015. MEDICINE. Global control of hepatitis C virus. Science 349:790-1.
4. Walker CM, Grakoui A. 2015. Hepatitis C virus: why do we need a vaccine to prevent a curable persistent infection? Curr Opin Immunol 35:137-43.
5. Fauvelle C, Colpitts CC, Keck ZY, Pierce BG, Foung SK, Baumert TF. 2016. Hepatitis C virus vaccine candidates inducing protective neutralizing antibodies. Expert Rev Vaccines doi:10.1080/14760584.2016.1194759:1-10.
6. Pierce BG, Keck ZY, Foung SK. 2016. Viral evasion and challenges of hepatitis C virus vaccine development. Curr Opin Virol 20:55-63.
7. Prentoe J, Verhoye L, Velazquez Moctezuma R, Buysschaert C, Farhoudi A, Wang R, Alter H, Meuleman P, Bukh J. 2015. HVR1-mediated antibody evasion of highly infectious in vivo adapted HCV in humanised mice. Gut doi:10.1136/gutjnl-2015-310300.
8. Morin TJ, Broering TJ, Leav BA, Blair BM, Rowley KJ, Boucher EN, Wang Y, Cheslock PS, Knauber M, Olsen DB, Ludmerer SW, Szabo G, Finberg RW, Purcell RH, Lanford RE, Ambrosino DM, Molrine DC, Babcock GJ. 2012. Human Monoclonal Antibody HCV1 Effectively Prevents and Treats HCV Infection in Chimpanzees. PLoS pathogens 8:e1002895.
9. Keck ZY, Li SH, Xia J, von Hahn T, Balfe P, McKeating JA, Witteveldt J, Patel AH, Alter H, Rice CM, Foung SK. 2009. Mutations in hepatitis C virus E2 located outside the CD81 binding sites lead to escape from broadly neutralizing antibodies but compromise virus infectivity. J Virol 83:6149-60.
10. Chung RT, Gordon FD, Curry MP, Schiano TD, Emre S, Corey K, Markmann JF, Hertl M, Pomposelli JJ, Pomfret EA, Florman S, Schilsky M, Broering TJ, Finberg RW, Szabo G, Zamore PD, Khettry U, Babcock GJ, Ambrosino DM, Leav B, Leney M, Smith HL, Molrine DC. 2013. Human monoclonal antibody MBL-HCV1 delays HCV viral rebound following liver transplantation: a randomized controlled study. Am J Transplant 13:1047-54.
11. Babcock GJ, Iyer S, Smith HL, Wang Y, Rowley K, Ambrosino DM, Zamore PD, Pierce BG, Molrine DC, Weng Z. 2014. High-throughput sequencing analysis of post-liver transplantation HCV E2 glycoprotein evolution in the presence and absence of neutralizing monoclonal antibody. PLoS One 9:e100325.
12. Impagliazzo A, Milder F, Kuipers H, Wagner MV, Zhu X, Hoffman RM, van Meersbergen R, Huizingh J, Wanningen P, Verspuij J, de Man M, Ding Z, Apetri A, Kukrer B, Sneekes-Vriese E, Tomkiewicz D, Laursen NS, Lee PS, Zakrzewska A, Dekking L, Tolboom J, Tettero L, van Meerten S, Yu W, Koudstaal W, Goudsmit J, Ward AB, Meijberg W, Wilson IA, Radosevic K. 2015. A stable trimeric influenza hemagglutinin stem as a broadly protective immunogen. Science 349:1301-6.
13. Yassine HM, Boyington JC, McTamney PM, Wei CJ, Kanekiyo M, Kong WP, Gallagher JR, Wang L, Zhang Y, Joyce MG, Lingwood D, Moin SM, Andersen H, Okuno Y, Rao SS, Harris AK, Kwong PD, Mascola JR, Nabel GJ, Graham BS. 2015. Hemagglutinin-stem nanoparticles generate heterosubtypic influenza protection. Nat Med 21:1065-70.

14. de Taeye SW, Ozorowski G, Torrents de la Pena A, Guttman M, Julien JP, van den Kerkhof TL, Burger JA, Pritchard LK, Pugach P, Yasmeen A, Crampton J, Hu J, Bontjer I, Torres JL, Arendt H, DeStefano J, Koff WC, Schuitemaker H, Eggink D, Berkhout B, Dean H, LaBranche C, Crotty S, Crispin M, Montefiori DC, Klasse PJ, Lee KK, Moore JP, Wilson IA, Ward AB, Sanders RW. 2015. Immunogenicity of Stabilized HIV-1 Envelope Trimers with Reduced Exposure of Non-neutralizing Epitopes. Cell 163:1702-15.
15. Kulp DW, Steichen JM, Pauthner M, Hu X, Schiffner T, Liguori A, Cottrell CA, Havenar-Daughton C, Ozorowski G, Georgeson E, Kalyuzhniy O, Willis JR, Kubitz M, Adachi Y, Reiss SM, Shin M, de Val N, Ward AB, Crotty S, Burton DR, Schief WR. 2017. Structure-based design of native-like HIV-1 envelope trimers to silence non-neutralizing epitopes and eliminate CD4 binding. Nat Commun 8:1655.
16. Joyce MG, Zhang B, Ou L, Chen M, Chuang GY, Druz A, Kong WP, Lai YT, Rundlet EJ, Tsybovsky Y, Yang Y, Georgiev IS, Guttman M, Lees CR, Pancera M, Sastry M, Soto C, Stewart-Jones GB, Thomas PV, Van Galen JG, Baxa U, Lee KK, Mascola JR, Graham BS, Kwong PD. 2016. Iterative structure-based improvement of a fusion-glycoprotein vaccine against RSV. Nat Struct Mol Biol 23:811-20.
17. Correia BE, Bates JT, Loomis RJ, Baneyx G, Carrico C, Jardine JG, Rupert P, Correnti C, Kalyuzhniy O, Vittal V, Connell MJ, Stevens E, Schroeter A, Chen M, Macpherson S, Serra AM, Adachi Y, Holmes MA, Li Y, Klevit RE, Graham BS, Wyatt RT, Baker D, Strong RK, Crowe JE, Jr., Johnson PR, Schief WR. 2014. Proof of principle for epitope-focused vaccine design. Nature 507:201-6.
18. Khera T, Behrendt P, Bankwitz D, Brown RJP, Todt D, Doepke M, Khan AG, Schulze K, Law J, Logan M, Hockman D, Wong JAJ, Dold L, Gonzalez-Motos V, Spengler U, Viejo-Borbolla A, Stroh LJ, Krey T, Tarr AW, Steinmann E, Manns MP, Klein F, Guzman CA, Marcotrigiano J, Houghton M, Pietschmann T. 2019. Functional and immunogenic characterization of diverse HCV glycoprotein E2 variants. J Hepatol 70:593-602.
19. Urbanowicz RA, Wang R, Schiel JE, Keck ZY, Kerzic MC, Lau P, Rangarajan S, Garagusi KJ, Tan L, Guest JD, Ball JK, Pierce BG, Mariuzza RA, Foung SKH, Fuerst TR. 2019. Antigenicity and Immunogenicity of Differentially Glycosylated Hepatitis C Virus E2 Envelope Proteins Expressed in Mammalian and Insect Cells. J Virol 93.
20. Vietheer PT, Boo I, Gu J, McCaffrey K, Edwards S, Owczarek C, Hardy MP, Fabri L, Center RJ, Poumbourios P, Drummer HE. 2017. The core domain of hepatitis C virus glycoprotein E2 generates potent cross-neutralizing antibodies in guinea pigs. Hepatology 65:1117-1131.
21. Law JLM, Logan M, Wong J, Kundu J, Hockman D, Landi A, Chen C, Crawford K, Wininger M, Johnson J, Mesa Prince C, Dudek E, Mehta N, Tyrrell DL, Houghton M. 2018. Role of the E2 Hypervariable Region (HVR1) in the Immunogenicity of a Recombinant Hepatitis C Virus Vaccine. J Virol 92.
22. He L, Cheng Y, Kong L, Azadnia P, Giang E, Kim J, Wood MR, Wilson IA, Law M, Zhu J. 2015. Approaching rational epitope vaccine design for hepatitis C virus with meta-server and multivalent scaffolding. Sci Rep 5:12501.
23. Pierce BG, Boucher EN, Piepenbrink KH, Ejemel M, Rapp CA, Thomas WD, Jr., Sundberg EJ, Weng Z, Wang Y. 2017. Structure-Based Design of Hepatitis C Virus

Vaccines That Elicit Neutralizing Antibody Responses to a Conserved Epitope. J Virol 91:e01032-17.
24. Keck ZY, Xia J, Wang Y, Wang W, Krey T, Prentoe J, Carlsen T, Li AY, Patel AH, Lemon SM, Bukh J, Rey FA, Foung SK. 2012. Human monoclonal antibodies to a novel cluster of conformational epitopes on HCV E2 with resistance to neutralization escape in a genotype 2a isolate. PLoS Pathog 8:e1002653.
25. Keck ZY, Op De Beeck A, Hadlock KG, Xia J, Li TK, Dubuisson J, Foung SK. 2004. Hepatitis C virus E2 has three immunogenic domains containing conformational epitopes with distinct properties and biological functions. J Virol 78:9224-32.
26. Keck ZY, Li TK, Xia J, Bartosch B, Cosset FL, Dubuisson J, Foung SK. 2005. Analysis of a highly flexible conformational immunogenic domain a in hepatitis C virus E2. J Virol 79:13199-208.
27. Kong L, Lee DE, Kadam RU, Liu T, Giang E, Nieusma T, Garces F, Tzarum N, Woods VL, Jr., Ward AB, Li S, Wilson IA, Law M. 2016. Structural flexibility at a major conserved antibody target on hepatitis C virus E2 antigen. Proc Natl Acad Sci U S A doi:10.1073/pnas.1609780113.
28. Pierce BG, Keck ZY, Lau P, Fauvelle C, Gowthaman R, Baumert TF, Fuerst TR, Mariuzza RA, Foung SKH. 2016. Global mapping of antibody recognition of the hepatitis C virus E2 glycoprotein: Implications for vaccine design. Proc Natl Acad Sci U S A 113:E6946-E6954.
29. Eggink D, Goff PH, Palese P. 2014. Guiding the immune response against influenza virus hemagglutinin toward the conserved stalk domain by hyperglycosylation of the globular head domain. J Virol 88:699-704.
30. Ringe RP, Ozorowski G, Rantalainen K, Struwe WB, Matthews K, Torres JL, Yasmeen A, Cottrell CA, Ketas TJ, LaBranche CC, Montefiori DC, Cupo A, Crispin M, Wilson IA, Ward AB, Sanders RW, Klasse PJ, Moore JP. 2017. Reducing V3 Antigenicity and Immunogenicity on Soluble, Native-Like HIV-1 Env SOSIP Trimers. J Virol 91.
31. Keck ZY, Wang Y, Lau P, Lund G, Rangarajan S, Fauvelle C, Liao GC, Holtsberg FW, Warfield KL, Aman MJ, Pierce BG, Fuerst TR, Bailey JR, Baumert TF, Mariuzza RA, Kneteman NM, Foung SK. 2016. Affinity maturation of a broadly neutralizing human monoclonal antibody that prevents acute hepatitis C virus infection in mice. Hepatology 64:1922-1933.
32. Krey T, Meola A, Keck ZY, Damier-Piolle L, Foung SK, Rey FA. 2013. Structural basis of HCV neutralization by human monoclonal antibodies resistant to viral neutralization escape. PLoS Pathog 9:e1003364.
33. Kinchen VJ, Cox AL, Bailey JR. 2018. Can Broadly Neutralizing Monoclonal Antibodies Lead to a Hepatitis C Virus Vaccine? Trends Microbiol 26:854-864.
34. Keck ZY, Girard-Blanc C, Wang W, Lau P, Zuiani A, Rey FA, Krey T, Diamond MS, Foung SK. 2016. Antibody Response to Hypervariable Region 1 Interferes with Broadly Neutralizing Antibodies to Hepatitis C Virus. J Virol 90:3112-22.
35. Gopal R, Jackson K, Tzarum N, Kong L, Ettenger A, Guest J, Pfaff JM, Barnes T, Honda A, Giang E, Davidson E, Wilson IA, Doranz BJ, Law M. 2017. Probing the antigenicity of hepatitis C virus envelope glycoprotein complex by high-throughput mutagenesis. PLoS Pathog 13:e1006735.

36. Tzarum N, Giang E, Kong L, He L, Prentoe J, Augestad E, Hua Y, Castillo S, Lauer GM, Bukh J, Zhu J, Wilson IA, Law M. 2019. Genetic and structural insights into broad neutralization of hepatitis C virus by human VH1-69 antibodies. Sci Adv 5:eaav1882.
37. Flyak AI, Ruiz S, Colbert MD, Luong T, Crowe JE, Jr., Bailey JR, Bjorkman PJ. 2018. HCV Broadly Neutralizing Antibodies Use a CDRH3 Disulfide Motif to Recognize an E2 Glycoprotein Site that Can Be Targeted for Vaccine Design. Cell Host Microbe 24:703-716 e3.
38. Li Y, Pierce BG, Wang Q, Keck ZY, Fuerst TR, Foung SK, Mariuzza RA. 2015. Structural basis for penetration of the glycan shield of hepatitis C virus E2 glycoprotein by a broadly neutralizing human antibody. J Biol Chem 290:10117-25.
39. Kong L, Giang E, Robbins JB, Stanfield RL, Burton DR, Wilson IA, Law M. 2012. Structural basis of hepatitis C virus neutralization by broadly neutralizing antibody HCV1. Proceedings of the National Academy of Sciences of the United States of America 109:9499-504.
40. Urbanowicz RA, McClure CP, Brown RJ, Tsoleridis T, Persson MA, Krey T, Irving WL, Ball JK, Tarr AW. 2015. A Diverse Panel of Hepatitis C Virus Glycoproteins for Use in Vaccine Research Reveals Extremes of Monoclonal Antibody Neutralization Resistance. J Virol 90:3288-301.
41. Prentoe J, Bukh J. 2018. Hypervariable Region 1 in Envelope Protein 2 of Hepatitis C Virus: A Linchpin in Neutralizing Antibody Evasion and Viral Entry. Front Immunol 9:2146.
42. Prentoe J, Velazquez-Moctezuma R, Augestad EH, Galli A, Wang R, Law M, Alter H, Bukh J. 2019. Hypervariable region 1 and N-linked glycans of hepatitis C regulate virion neutralization by modulating envelope conformations. Proc Natl Acad Sci U S A 116:10039-10047.
43. Law M, Maruyama T, Lewis J, Giang E, Tarr AW, Stamataki Z, Gastaminza P, Chisari FV, Jones IM, Fox RI, Ball JK, McKeating JA, Kneteman NM, Burton DR. 2008. Broadly neutralizing antibodies protect against hepatitis C virus quasispecies challenge. Nat Med 14:25-7.
44. Li D, von Schaewen M, Wang X, Tao W, Zhang Y, Li L, Heller B, Hrebikova G, Deng Q, Ploss A, Zhong J, Huang Z. 2016. Altered Glycosylation Patterns Increase Immunogenicity of a Subunit Hepatitis C Virus Vaccine, Inducing Neutralizing Antibodies Which Confer Protection in Mice. J Virol 90:10486-10498.
45. Bailey JR, Flyak AI, Cohen VJ, Li H, Wasilewski LN, Snider AE, Wang S, Learn GH, Kose N, Loerinc L, Lampley R, Cox AL, Pfaff JM, Doranz BJ, Shaw GM, Ray SC, Crowe JE, Jr. 2017. Broadly neutralizing antibodies with few somatic mutations and hepatitis C virus clearance. JCI Insight 2.
46. Merat SJ, Molenkamp R, Wagner K, Koekkoek SM, van de Berg D, Yasuda E, Bohne M, Claassen YB, Grady BP, Prins M, Bakker AQ, de Jong MD, Spits H, Schinkel J, Beaumont T. 2016. Hepatitis C virus Broadly Neutralizing Monoclonal Antibodies Isolated 25 Years after Spontaneous Clearance. PLoS One 11:e0165047.
47. Stejskal L, Lees WD, Moss DS, Palor M, Bingham RJ, Shepherd AJ, Grove J. 2020. Flexibility and intrinsic disorder are conserved features of hepatitis C virus E2 glycoprotein. PLoS Comput Biol 16:e1007710.
48. Sanders RW, Derking R, Cupo A, Julien JP, Yasmeen A, de Val N, Kim HJ, Blattner C, de la Pena AT, Korzun J, Golabek M, de Los Reyes K, Ketas TJ, van Gils MJ, King CR,

Wilson IA, Ward AB, Klasse PJ, Moore JP. 2013. A next-generation cleaved, soluble HIV-1 Env trimer, BG505 SOSIP.664 gp140, expresses multiple epitopes for broadly neutralizing but not non-neutralizing antibodies. PLoS Pathog 9:e1003618.
49. Krarup A, Truan D, Furmanova-Hollenstein P, Bogaert L, Bouchier P, Bisschop IJM, Widjojoatmodjo MN, Zahn R, Schuitemaker H, McLellan JS, Langedijk JPM. 2015. A highly stable prefusion RSV F vaccine derived from structural analysis of the fusion mechanism. Nat Commun 6:8143.
50. Pallesen J, Wang N, Corbett KS, Wrapp D, Kirchdoerfer RN, Turner HL, Cottrell CA, Becker MM, Wang L, Shi W, Kong WP, Andres EL, Kettenbach AN, Denison MR, Chappell JD, Graham BS, Ward AB, McLellan JS. 2017. Immunogenicity and structures of a rationally designed prefusion MERS-CoV spike antigen. Proc Natl Acad Sci U S A 114:E7348-E7357.
51. Wrapp D, Wang N, Corbett KS, Goldsmith JA, Hsieh CL, Abiona O, Graham BS, McLellan JS. 2020. Cryo-EM structure of the 2019-nCoV spike in the prefusion conformation. Science 367:1260-1263.
52. Sullivan JT, Sulli C, Nilo A, Yasmeen A, Ozorowski G, Sanders RW, Ward AB, Klasse PJ, Moore JP, Doranz BJ. 2017. High-Throughput Protein Engineering Improves the Antigenicity and Stability of Soluble HIV-1 Envelope Glycoprotein SOSIP Trimers. J Virol 91.
53. Pierce BG, Hellman LM, Hossain M, Singh NK, Vander Kooi CW, Weng Z, Baker BM. 2014. Computational design of the affinity and specificity of a therapeutic T cell receptor. PLoS Comput Biol 10:e1003478.
54. Anderson RJ, Weng Z, Campbell RK, Jiang X. 2005. Main-chain conformational tendencies of amino acids. Proteins 60:679-89.
55. Kortemme T, Baker D. 2002. A simple physical model for binding energy hot spots in protein-protein complexes. Proc Natl Acad Sci U S A 99:14116-21.
56. Bohne-Lang A, von der Lieth CW. 2005. GlyProt: in silico glycosylation of proteins. Nucleic acids research 33:W214-9.
57. Hubbard SJ, Thornton JM. 1993. NACCESS, v2.1.1. Department of Biochemistry and Molecular Biology, University College London,
58. Wen B, Deng Y, Guan J, Yan W, Wang Y, Tan W, Gao J. 2011. Signal peptide replacements enhance expression and secretion of hepatitis C virus envelope glycoproteins. Acta Biochim Biophys Sin (Shanghai) 43:96-102.
59. Keck Z, Wang W, Wang Y, Lau P, Carlsen TH, Prentoe J, Xia J, Patel AH, Bukh J, Foung SK. 2013. Cooperativity in virus neutralization by human monoclonal antibodies to two adjacent regions located at the amino terminus of hepatitis C virus E2 glycoprotein. J Virol 87:37-51.
60. Keck ZY, Saha A, Xia J, Wang Y, Lau P, Krey T, Rey FA, Foung SK. 2011. Mapping a region of hepatitis C virus E2 that is responsible for escape from neutralizing antibodies and a core CD81-binding region that does not tolerate neutralization escape mutations. J Virol 85:10451-63.
61. Hadlock KG, Lanford RE, Perkins S, Rowe J, Yang Q, Levy S, Pileri P, Abrignani S, Foung SK. 2000. Human monoclonal antibodies that inhibit binding of hepatitis C virus E2 protein to CD81 and recognize conserved conformational epitopes. J Virol 74:10407-16.

769 62. Andrianov AK, Svirkin YY, LeGolvan MP. 2004. Synthesis and biologically relevant
770 properties of polyphosphazene polyacids. Biomacromolecules 5:1999-2006.
771 63. Andrianov AK, Marin A, Fuerst TR. 2016. Molecular-Level Interactions of
772 Polyphosphazene Immunoadjuvants and Their Potential Role in Antigen Presentation and
773 Cell Stimulation. Biomacromolecules 17:3732-3742.
774 64. Kong L, Giang E, Nieusma T, Kadam RU, Cogburn KE, Hua Y, Dai X, Stanfield RL,
775 Burton DR, Ward AB, Wilson IA, Law M. 2013. Hepatitis C virus E2 envelope
776 glycoprotein core structure. Science 342:1090-4.
777 65. Kortemme T, Kim DE, Baker D. 2004. Computational alanine scanning of protein-
778 protein interfaces. Sci STKE 2004:pl2.
779 66. Owsianka A, Tarr AW, Juttla VS, Lavillette D, Bartosch B, Cosset FL, Ball JK, Patel
780 AH. 2005. Monoclonal antibody AP33 defines a broadly neutralizing epitope on the
781 hepatitis C virus E2 envelope glycoprotein. J Virol 79:11095-104.
782

783

784

Figure Legends

Figure 1. Structure-based design of E2 to stabilize and mask epitopes. A) Design of the E2 front layer. (top) Antigenic domain B-D supersite (green; also referred to as antigenic region 3) is highlighted on the E2 core X-ray structure (64), along with antigenic domain E (blue), and modeled N-glycans shown as orange sticks. Ramachandran plot analysis for proline-like backbone conformation (middle) and structural modeling of proline substitution structural and energetic effects (bottom) were performed using RosettaDesign and the HC84.26.5D-AS434 epitope complex structure (31). HC84.26.5D HMAb is shown as wheat and light blue surface, epitope is green with selected mutant residue (H445P) shown as sticks. B) Design of the E2 back layer. (top) Antigenic domain A (red) was targeted for design and is shown on the E2 core structure, and antigenic domain C and modeled N-glycans are shown in cyan and orange sticks, respectively. (middle) Computational N-glycan scanning of antigenic domain A residues was performed to identify substitutions to mask its surface with designed NxS and NxT sequons. (bottom) Modeling of sequon mutants was performed in Rosetta (65), followed by modeling of N-glycan structures in the Glyprot Server (56). Modeled N-glycan design at Y632 (Y632N-G634S) shown as green sticks, with E2 core structure gray (based on H77C E2, PDB code 4MWF), E2 antigenic domain A residues red, and modeled native E2 N-glycans light blue sticks.

Figure 2. Antigenic characterization of E2 designs using ELISA. Designs were cloned and expressed in the context of E1E2 as previously described (28) and tested for binding to a panel of HMAbs that target E2 antigenic domain A (CBH-4G, CBH-4B), B (HC-1), C (CBH-7), D (HC84.28, HC84.24, HC84.26), and E (HC33.1, HC33.4), at concentrations of 1 μg/ml, and 5 μg/ml. Binding was tested to wild-type H77C E1E2, and compared with designs ΔHVR1 (E2

residues 384-407 deleted), $\Delta HVR1_{411}$ (E2 residues 384-410 deleted), H445P, F627NT (F627N-V629T), R630NT (R630N-Y632T), K628NS (K628N-R630S), and Y632NS (Y632N-G634S). Asterisks denote designs that were tested in the context of $\Delta HVR1_{411}$ (E2 residues 384-410 deleted) rather than full length E1E2.

Figure 3. Antigenic characterization of sE2 designs H445P and Y632NS using biolayer interferometry (BLI). (A) Measured binding of broadly neutralizing monoclonal antibody HC84.26.WH.5DL to E2 design H445P compared to wild-type soluble E2 (sE2). (B) Measured binding of non-neutralizing monoclonal antibody CBH-4G to E2 design Y632NS (Y632N-G634S) compared to wild-type soluble E2 (sE2). Steady-state binding curve fits are shown, which were used to determine binding dissociation constants (K_d) values.

Figure 4. Immunized serum recognition of E2 and two E2 epitopes. A) Immunized sera were tested using ELISA for binding to soluble H77C E2 (sE2) and linear epitopes from antigenic domain E (AS412, aa 410-425) and antigenic domain D (AS434, aa 434-446). Serum binding was tested at successive three-fold dilutions starting at 1:60, and values are reported as endpoint titers. B) Binding of peptides to control monoclonal antibodies HC33.1 (59), AP33 (66), and HC84.26.WH.5DL (31).

Figure 5. Serum binding competition with monoclonal antibodies. Serum inhibition of binding by biotinylated monoclonal antibodies at a concentration of 1 µg/ml was tested at the serum dilutions shown, using ELISA. The monoclonal antibodies tested for serum competition target E2 antigenic domains A (CBH-4G), B (HC-1), and D (HC84.26).

Figure 6. Immunized serum binding to recombinant E1E2 and HCV pseudoparticles (HCVpp). Immunized sera were tested for binding to (A) H77C E1E2, and HCVpp representing (B) H77C, (C) UKNP1.18.1, and (D) J6 isolates using ELISA. Serum binding was tested at three-fold dilutions starting at 1:100, and values are reported as endpoint titers. Murine sera with binding levels lower than the endpoint OD value at the minimum dilution (1:100) have titers shown as 50. Due to insufficient sera, endpoint titers are not available for one mouse in the sE2 group and one mouse in ΔHVR1 group (E1E2, H77C HCVpp, J6 HCVpp), as well as two mice in the sE2 group and one mouse in the ΔHVR1-Y632NS group (UKNP1.18.1 HCVpp). P-values between group endpoint titer values were calculated using Kruskal-Wallis analysis of variance with Dunn's multiple comparison test, and significant p-values between sE2 control and sE2 design groups are shown (*: $p \leq 0.05$; ****: $p \leq 0.0001$).

Figure 7. Comparison of concentrated HCV pseudoparticle (HCVpp) binding of immunized mouse sera from sE2 wild-type and H445P immunization. A preparation enriched in H77C HCVpps was tested for binding to pooled murine sera from sE2 wild-type and H445P groups using ELISA, for sera from Day 42 and Day 56. Best-fit curves are shown and were used to calculate EC50 values.

Figure 8. Binding of concentrated HCV pseudoparticles (HCVpps), pseudotyped with H77C E1E2, to monoclonal antibodies. Binding measurements were performed using ELISA with antibodies targeting E2 (HCV1, HC84.26.WH.5DL, AR3A), E1E2 (AR4A, AR5A) and a negative control antibody (CA45).

Figure 9. Serum neutralization of homologous (H77C) and heterologous HCVpp. Immunized murine serum neutralization was tested using HCV pseudoparticles (HCVpps) representing H77C as well as six heterologous isolates. Neutralization for four HCVpp representing isolates with resistant phenotypes are shown on the right, as indicated. Neutralization titers are represented as serum dilution levels required to reach 50% virus neutralization (ID50), calculated by curve fitting in Graphpad Prism software. Serum dilutions were performed as two-fold dilutions starting at 1:64, and minimum dilution levels (corresponding to 1:64) are indicated as dotted lines for reference. Murine sera with low (calculated ID50 < 10) or incalculable ID50 values due to low or background levels of neutralization (observed only for some mice for J6 HCVpp neutralization) have ID50 shown as 10. Due to insufficient sera, J6 neutralization measurements did not include two mice from group 1 (sE2) and one mouse from group 4 (ΔHVR1). P-values between group ID50 values were calculated using Kruskal-Wallis analysis of variance with Dunn's multiple comparison test, and significant p-values between sE2 control and sE2 design groups are shown (*: $p \leq 0.05$; **: $p \leq 0.01$).

Figure 10. Analysis of correlations in immunogenicity and antigenicity measurements. (A) Pairs of datasets of serum HCVpp neutralization (IC50) and antigen binding (endpoint titer) measurements were tested for Pearson correlations on an individual mouse level (42 points per dataset), and top correlations between datasets are shown. Pearson correlations were calculated using log-transformed ID50 and endpoint titer values. (B) UKNP2.4.1 versus UKNP1.18.1 serum neutralization (ID50), with best-fit line in red, and calculated correlation (r) and p-value (p) shown. (C) Correlations between antigen binding (K_d) and immunogenicity measurements for

corresponding antigen group (group geometric mean ID50 or endpoint titer) were calculated, and most significant correlations are shown. Pearson correlations were calculated using negated log-transformed K_d and log-transformed titer values. (D) UKNP1.18.1 group serum neutralization (ID50) versus HC84.26.WH.5DL HMAb affinity (K_d), with best-fit line in red, and calculated correlation (r) and p-value (p) shown. The log-scale x-axis for HC84.26.WH.5DL K_d is shown with reversed scale, in accordance with the polarity of the calculated correlation. For (A) and (C), correlation p-values are shown above each bar (*: $p \leq 0.05$; **: $p \leq 0.01$, ***: $p \leq 0.001$, ****: $p \leq 0.0001$).

888 **Figure 1**.

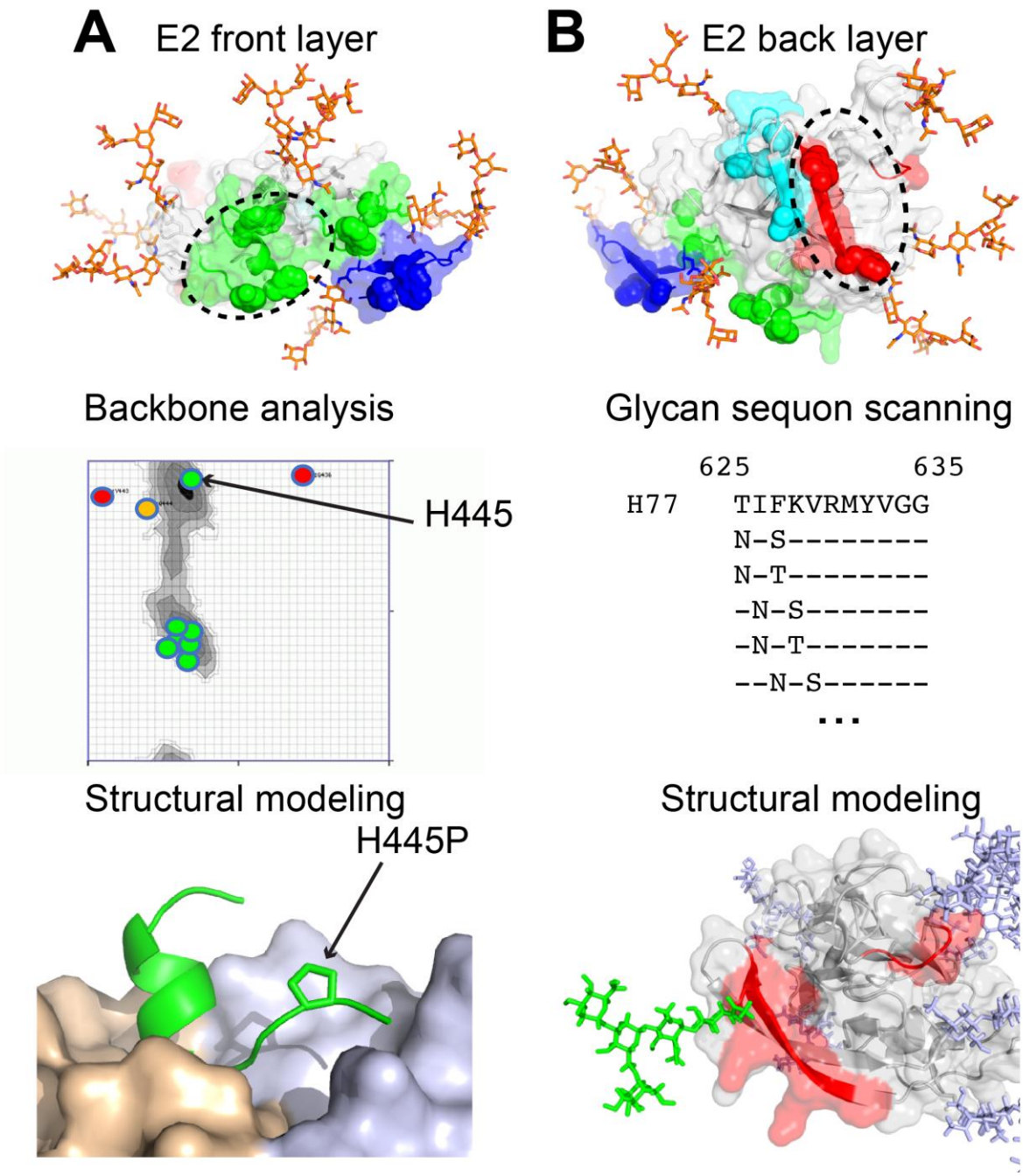

889

Figure 2.

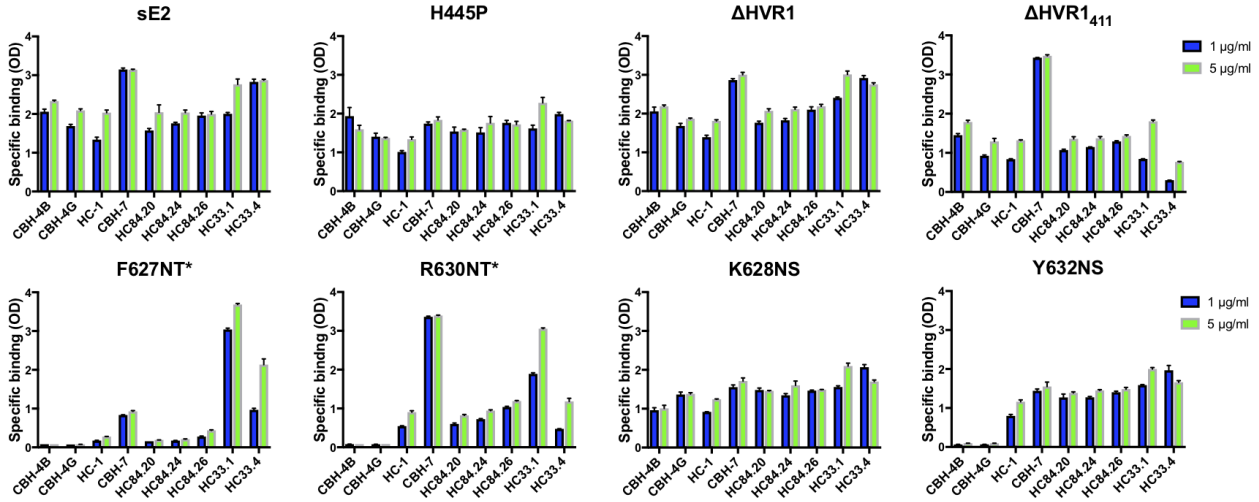
sE2
H445P
ΔHVR1
ΔHVR1411
F627NT*
R630NT*
K628NS
Y632NS
Specific bindng (OD)
1 µg/ml
5 µg/ml
CBH-4B
CBH-4G
HC-1
CBH-7
HC84.20
HC84.24
HC84.26
HC33.1
HC33.4

Figure 3.

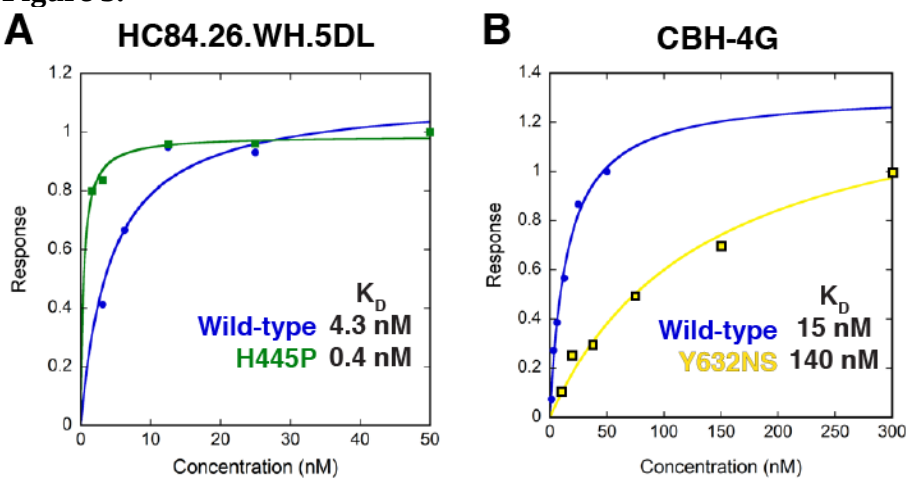
A
HC84.26.WH.5DL
Response
Concentration (nM)
K_D
Wild-type 4.3 nM
H445P 0.4 nM
B
CBH-4G
Response
Concentration (nM)
K_D
Wild-type 15 nM
Y632NS 140 nM

Figure 4.

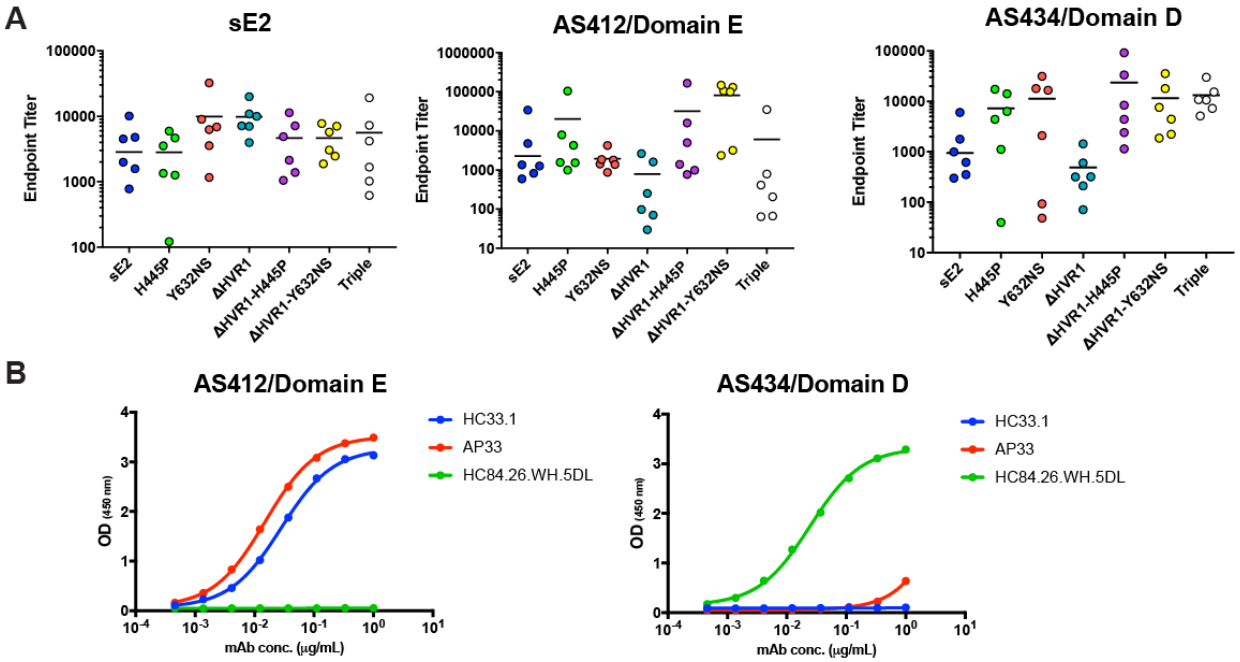
A
sE2
AS412/Domain E
AS434/Domain D
Endpoint Titer
sE2
H445P
Y632NS
ΔHVR1
ΔHVR1-H445P
ΔHVR1-Y632NS
Triple
B
AS412/Domain E
AS434/Domain D
OD (450 nm)
mAb conc. (μg/mL)
HC33.1
AP33
HC84.26.WH.5DL

Figure 5.

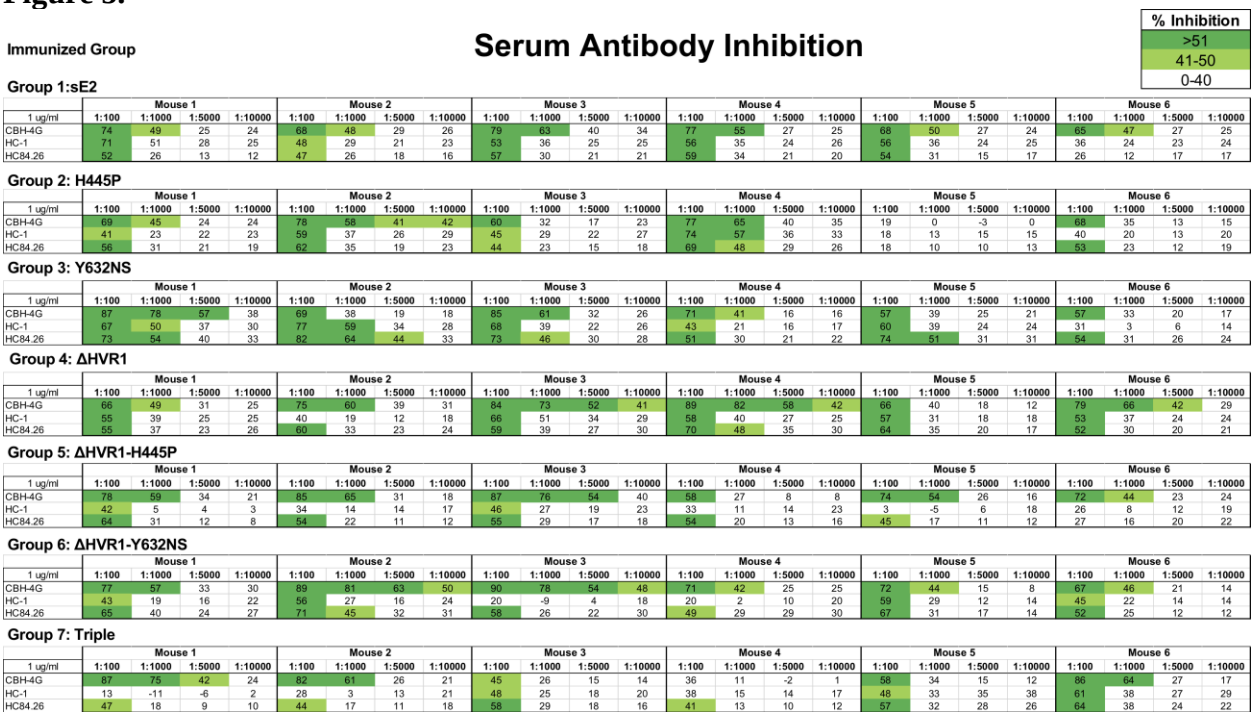
Immunized Group
Serum Antibody Inhibition
% Inhibition
>51
41-50
0-40
Group 1:sE2
Group 2: H445P
Group 3: Y632NS
Group 4: ΔHVR1
Group 5: ΔHVR1-H445P
Group 6: ΔHVR1-Y632NS
Group 7: Triple
Mouse 1
Mouse 2
Mouse 3
Mouse 4
Mouse 5
Mouse 6
1 ug/ml
1:100
1:1000
1:5000
1:10000
CBH-4G
HC-1
HC84.26

Figure 6.

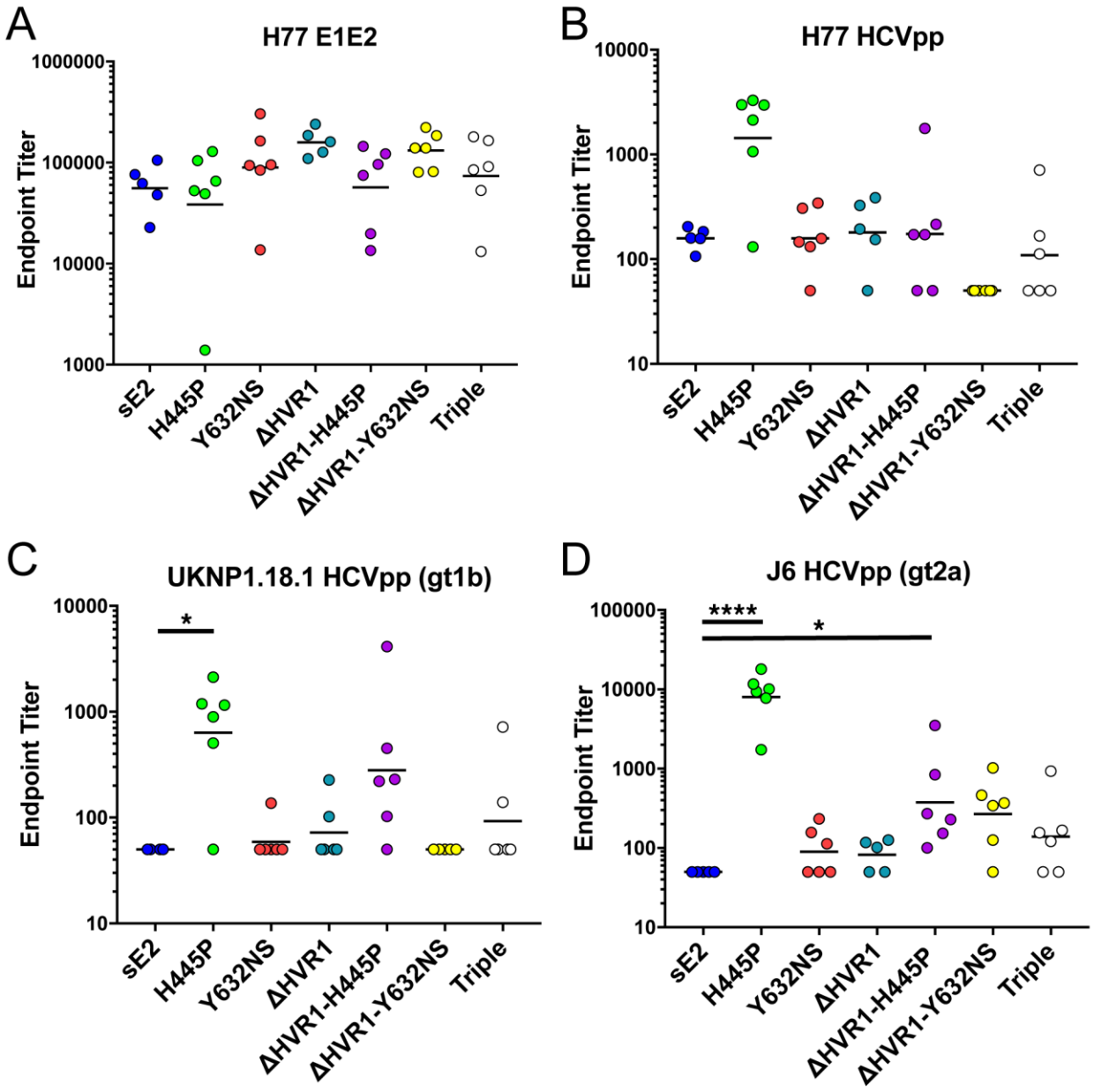
A
H77 E1E2
Endpoint Titer
1000000
100000
10000
1000
sE2
H445P
Y632NS
ΔHVR1
ΔHVR1-H445P
ΔHVR1-Y632NS
Triple
B
H77 HCVpp
Endpoint Titer
10000
1000
100
10
C
UKNP1.18.1 HCVpp (gt1b)
*
D
J6 HCVpp (gt2a)
****
*

902 **Figure 7.**

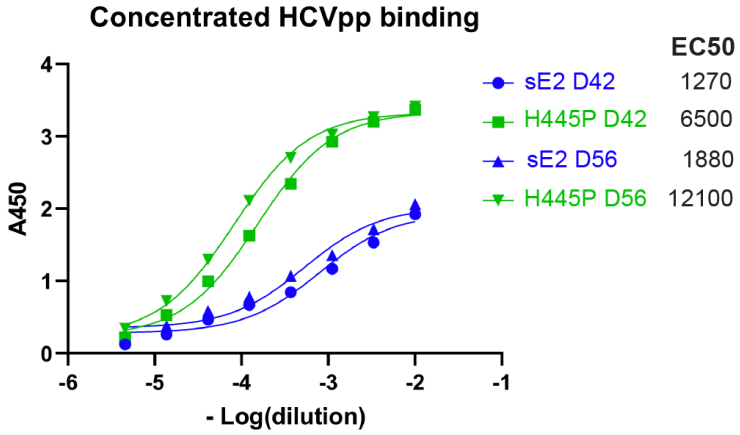

903
904

Figure 8.

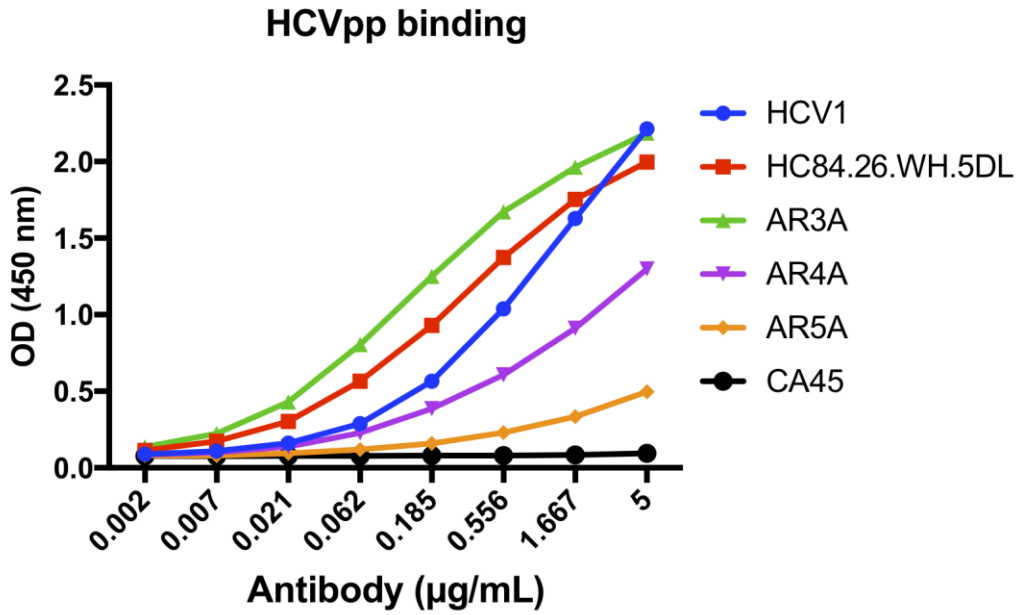
HCVpp binding
OD (450 nm)
2.5
2.0
1.5
1.0
0.5
0.0
0.002
0.007
0.021
0.062
0.185
0.556
1.667
5
Antibody (µg/mL)
HCV1
HC84.26.WH.5DL
AR3A
AR4A
AR5A
CA45

Figure 9.

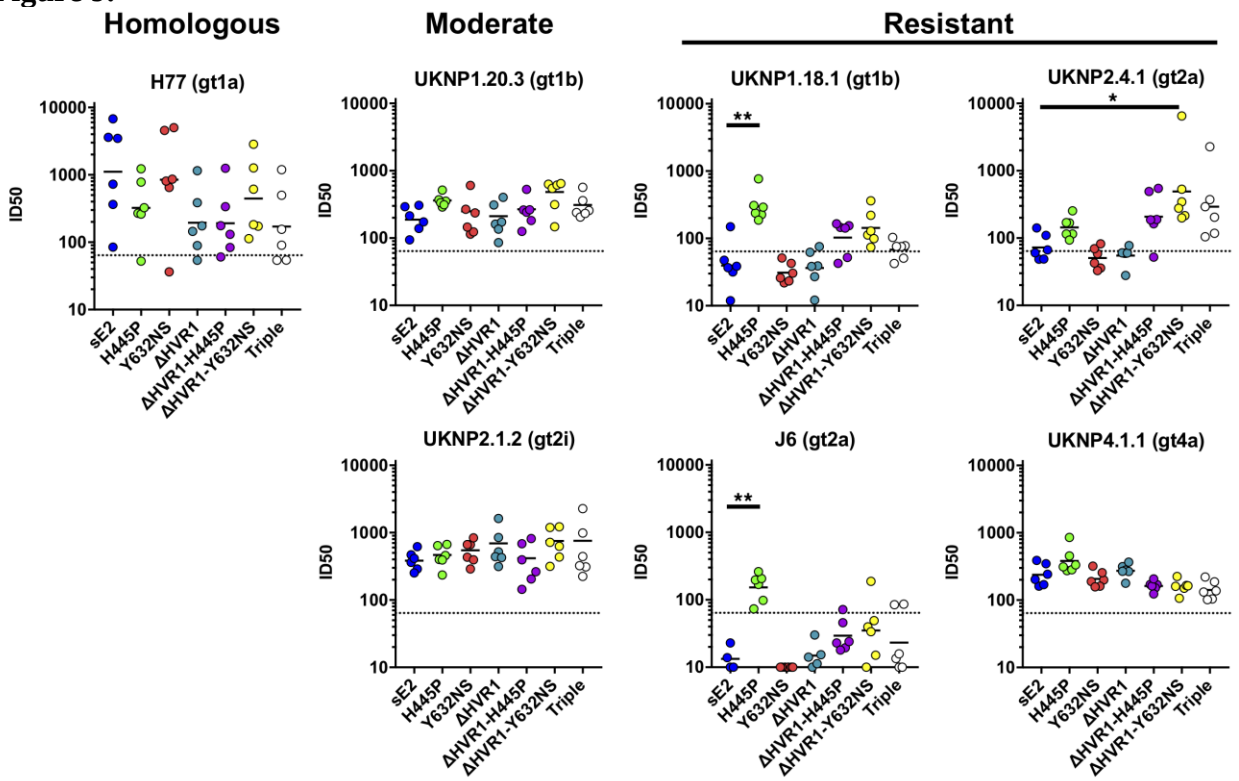
Homologous
Moderate
Resistant
H77 (gt1a)
UKNP1.20.3 (gt1b)
UKNP1.18.1 (gt1b)
UKNP2.4.1 (gt2a)
UKNP2.1.2 (gt2i)
J6 (gt2a)
UKNP4.1.1 (gt4a)
ID50
10000
1000
100
10
**
*
sE2
H445P
Y632NS
ΔHVR1
ΔHVR1-H445P
ΔHVR1-Y632NS
Triple

Figure 10.

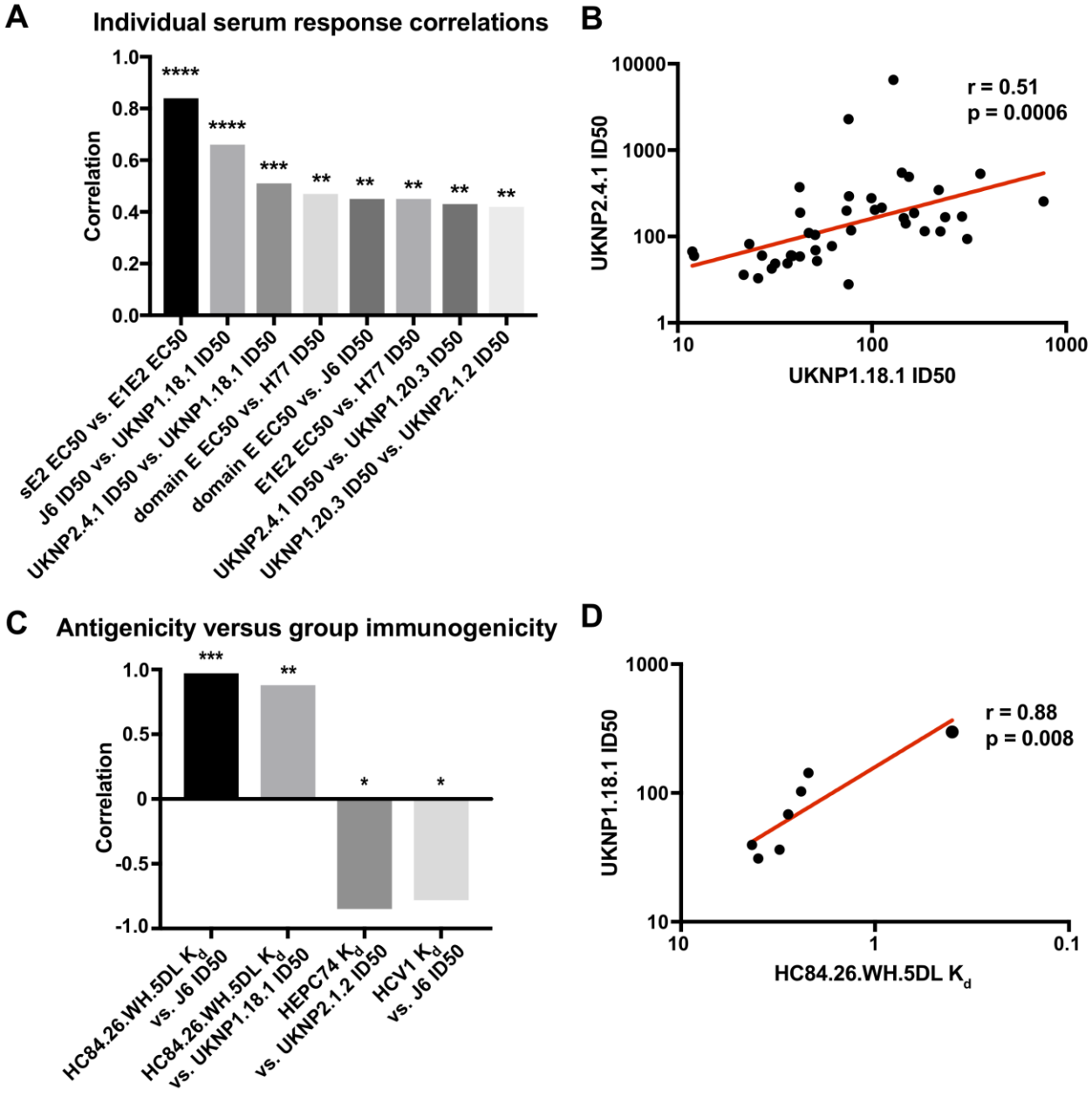
A
Individual serum response correlations
Correlation
1.0
0.8
0.6
0.4
0.2
0.0
****
****
***
**
**
**
**
**
sE2 EC50 vs. E1E2 EC50
J6 ID50 vs. UKNP1.18.1 ID50
UKNP2.4.1 ID50 vs. UKNP1.18.1 ID50
domain E EC50 vs. H77 ID50
domain E EC50 vs. J6 ID50
E1E2 EC50 vs. H77 ID50
UKNP2.4.1 ID50 vs. UKNP1.20.3 ID50
UKNP1.20.3 ID50 vs. UKNP2.1.2 ID50
B
UKNP2.4.1 ID50
10000
1000
100
1
10
100
1000
UKNP1.18.1 ID50
r = 0.51
p = 0.0006
C
Antigenicity versus group immunogenicity
Correlation
1.0
0.5
0
-0.5
-1.0
***
**
*
*
HC84.26.WH.5DL Kd vs. J6 ID50
HC84.26.WH.5DL Kd vs. UKNP1.18.1 ID50
HEPC74 Kd vs. UKNP2.1.2 ID50
HCV1 Kd vs. J6 ID50
D
UKNP1.18.1 ID50
1000
100
10
10
1
0.1
HC84.26.WH.5DL Kd
r = 0.88
p = 0.008

Table 1. Backbone structure and proline mutant analysis of antigenic domain D residues.

		Backbone angles[1]		Backbone analysis[1]		
Residue	**Wild-type aa**	**Φ, °**	**Ψ, °**	**Pro**	**Pre-Pro**	**Rosetta Proline ΔΔG[2]**
437	Trp	-73.66	-18.28	Yes	No	0.5
438	Leu	-59.18	-59.67	Yes	No	0.3
439	Ala	-59.14	-37.12	Yes	Yes	0
440	Gly	-56.62	-26.31	Yes	Yes	0.1
441	Leu	-68.3	-40.87	Yes	Yes	2.1
442	Phe	-80.55	-40.18	Yes	Yes	2.7
443	Tyr	-159.11	143.78	No	Yes	2.5
444	Gln	-110.46	128.63	No	Yes	2.2
445	His	-58.15	153.22	Yes	Yes	0

[1]Values and proline backbone analysis were obtained from the Ramachandran plot analysis web server (https://zlab.umassmed.edu/bu/rama/)(54). Pre-Pro assessments correspond to pre-proline Ramachandran plot conformation for the backbone of the preceding residue. Unfavorable Pro or Pre-Pro conformations are noted with gray shaded cells.

[2]Predicted binding energy change for proline epitope mutant to the HC84.26.5D HMAb, based on the X-ray structure of the complex (PDB code 4Z0X) and computational mutagenesis in Rosetta (55). Predicted destabilizing values (> 0.5 in Rosetta energy units) are indicated with shaded cells.

Table 2. Calculated surface accessibility of E2 residues in antigenic domain A.

Residue	Amino Acid	Side Chain ASA[1]
627	Phe	62.7
628	Lys	89.4
629	Val	38.4
630	Arg	60.4
631	Met	14
632	Tyr	62.3
633	Val	1.5

[1]Accessible surface areas calculated using the X-ray structure of H77 E2 core (PDB code 4MWF) and the naccess program (57) with default parameters. Values reflect relative side chain surface accessibility (normalized to 100).

Table 3. Antigenic and biophysical characterization of E2 designs.

		Antibody/Receptor Binding K_D, nM[3]								
		Domain A		Domain B		Domain D		Domain E		Receptor
sE2 Construct[1]	**T_m[2]**	**CBH-4D**	**CBH-4G**	**AR3A**	**HEPC74**	**HC84.26.WH.5DL**	**HC84.1**	**HCV1**	**HC33.1**	**CD81**
sE2 wild-type	84.5	8.4	15	1.8	5.1	4.3	30	42	9.5	22
H445P	83.1	14	15	1.1	4.6	**0.4**	31	70	8.0	23
Y632NS	81.4	37	**180**	1.2	4.6	4.0	83	26	6.5	31
ΔHVR1	84.5	5.8	20	1.5	7.0	3.1	60	42	7.9	15
ΔHVR1-H445P	82.9	11	15	1.5	2.3	2.4	51	46	7.6	10
ΔHVR1-Y632NS	80.0	7.7	**140**	1.8	9.0	2.2	110	50	6.7	**140**
Triple	76.5	22	**110**	1.4	4.6	2.8	58	27	9	40

[1]sE2 wild-type corresponds to residues 384-661 of H77C E2, and listed designs represent point mutants or truncations of that sequence. Y632NS is an abbreviation for the double mutant Y632N-G634S, and ΔHVR1 denotes deletion of most of the HVR1 sequence at the N-terminus of E2, with resultant construct containing residues 408-661. "Triple" denotes combination of ΔHVR1, H445P, and Y632NS designs.

[2]T_m values are in °C and were measured by differential scanning calorimetry.

[3]Steady-state dissociation constant (K_D) values were measured by Octet biolayer interferometry. Antibodies are classified by their mapping to antigenic domains A, B, D, and E on E2 (28). Values in bold denote K_D changes more than 5-fold versus wild-type E2 for that antibody.

Table 4. Percentage occupancy for engineered N-glycan at position 632, determined by mass spectrometry.

Design	% Glycosylation	EndoF Efficiency
Y632NS	51	96
ΔHVR1-Y632NS	44	97
Triple[1]	22	100

[1]Combination of ΔHVR1, H445P, and Y632NS.

945 **Table 5**. Panel of viral isolates used in neutralization assays.

Isolate	Genotype	Neutralization Phenotype	Neutralization Resistance Rank	% ID H77 sE2	% ID H77 ΔHVR1
H77	1a	Moderate	22	100	100
UKNP1.18.1	1b	Resistant	3	79	82
UKNP1.20.3	1b	Moderate	32	79	82
UKNP2.4.1	2a	Resistant	1	72	74
UKNP2.1.2	2i	Moderate	23	70	73
UKNP4.1.1	4a	Resistant	2	71	75
J6	2a	Resistant	11	71	74

946
947 [1]Neutralization phenotype and neutralization resistance rank based on assessment of 78 HCVpp
948 with a panel of monoclonal antibodies by Urbanowicz et al. (40).
949 [2]Percent identities reflect percent amino acid sequence identities with H77C sE2 (aa 384-661)
950 and ΔHVR1 (aa 408-661).